Biochimica et Biophysica Acta, 985 (1989) 60–66
Elsevier

BBAMEM 74579

The lipopeptide antibiotic A21978C has a specific interaction with DMPC only in the presence of calcium ions

Jeremy H. Lakey [1], Régine Maget-Dana [2] and Marius Ptak [2]

[1] *European Molecular Biology Laboratory, Heidelberg (F.R.G.) and* [2] *Centre de Biophysique Moléculaire (CNRS) and Université d'Orléans, Orléans (France)*

(Received 10 April 1989)

Key words: Lipopeptide antibiotic; A21978C; LY146032; Calcium dependence; Daptomycin; Dimyristoylphosphatidylcholine

The A21978C group are lipopeptide antibiotics which kill Gram-positive bacteria only in the presence of calcium ions. The calcium requirement of the antibacterial activity of A21978C correlates well with an in vitro calcium-dependent insertion into phospholipid vesicles. In this paper the interaction of A21978C with phosphatidylcholine is investigated in mixed monomolecular films. The spontaneity of the antibiotic-lipid mixing was determined by calculating the free energy change. On a Ca^{2+} containing subphase there is a specific interaction between the components at all antibiotic-lipid ratios. This is not true on K^+ subphases, where specific interactions never occur. On Mg^{2+} subphases specific interactions occur only in monolayers containing very little lipid. By analysing the fluorescence of the kynurenine residue we have followed the effects of two factors on the penetration of the antibiotic into lipid bilayer vesicles. Firstly, the phospholipid gel to liquid crystalline phase transition which in the absence of calcium leads to an exclusion of the antibiotic from the bilayer. This trend is completely reversed in the presence of Ca^{2+}. Secondly, the role of this lipopeptide's lipid tail was clarified by use of a series of versions of increasing fatty acyl chain length. The results indicate that the interaction promoted by calcium is not simply a hydrophobic attraction between fatty acyl chains but is more likely to be a specific interaction between polar headgroups.

Introduction

The A21978C series of antibiotics possess an intriguing antibacterial activity which is highly calcium dependent [1]. They are acidic lipopeptides produced by *Streptomyces roseosporus* and consist of an identical peptide attached to different fatty acyl tails [2]. Changing the length of these fatty chains has a marked effect on the antibacterial activity and the hemisynthetic LY146032 (decanoyl-A21978C, daptomycin) has been selected as the most promising version for clinical study. The site of action is not known, but Allen et al. [3] have shown that it inhibits a very early stage in peptidoglycan synthesis which may be cytoplasmic. Membrane activity is an important general feature of the action of lipopeptide antibiotics (iturins [4], amphomycin [5], bacitracin [6] and polymyxin [7]) and recently we have shown that A21978C binds to phospholipid membranes in a calcium-dependent manner by way of a calcium binding site on the peptide [8]. This activity was further clarified by the demonstration of a calcium dependent conformational change occurring in pure A21978C monolayers [9]. Previously described calcium dependent antibiotics (amphomycin [5,10], bacitracin [6]) act by binding to the phosphate groups of carrier lipids such as dolichol phosphate, but the study by Allen et al. [3] shows that this is not the site of action of A21978C. This article describes experiments which show that the membrane phospholipids themselves have a specific interaction with A21978C only in the presence of calcium ions.

Materials and Methods

A21978C and its derivatives were a gift from L.E. Day of Eli Lilly & Co. They consisted of A21978C_1 (*anteiso*-undecanoyl-A21978C), A21978C_2 (*iso*-dodecanoyl-A21978C), A21978C_3 (*anteiso*-tridecanoyl-A21978C) and LY146032 (decanoyl-A21978C) (see Ref. 2 for details of the chemical structure). Egg-yolk phosphatidylcholine (egg-PC) was purified according to the method of Singleton et al. [11] whilst DMPC was

Abbreviations: PC, phosphatidylcholine; SUV, small unilamellar vesicle; Kyn, Kynurenine; ANS, 8-anilinonaphthalene 1-sulphonate.

Correspondence: J.H. Lakey, European Molecular Laboratory, Postfach 10-2209, Meyerhofstrasse 1, 6900 Heidelberg, F.R.G.

purchased from Sigma, verified pure by thin layer chromatography and used without further purification. All other chemicals were of Analar grade or better. For the monolayer experiments pure water was obtained from a Millipore (Milli-Q) apparatus and the salt solutions (KCl, $MgCl_2$, $CaCl_2$) were treated with charcoal and subsequently filtered through a 0.2 μm polycarbonate membrane.

Small unilamellar vesicles (SUVs) were prepared by sonication. Phosphatidylcholine in ethanol was dried as a thin film inside a glass cup, a standard buffer solution added (200 mM KCl/10 mM cacodylate (pH 6.0)) and sonication was carried out under nitrogen by an MSE probe sonicator. Vesicles were then centrifuged for 1 h at 40000 rpm (Beckman 50 Ti rotor, 130000 × g) to remove multilamellar liposomes and titanium fragments. For egg-PC this was done at 0–5 °C whereas DMPC vesicles were always handled above 25 °C to avoid passing through the lipid phase transition. PC concentrations were determined by the method of Chen et al. [12].

Monolayer experiments

Monolayer measurements were made using a Langmuir film balance system previously described [13]. The antibiotic/lipid mixtures were dissolved in hexafluoroisopropanol/dioxane (5:1, v/v) and spread at the air/water interface with a 50 µl Hamilton microsyringe. The resulting monolayer was allowed to equilibrate at a large equivalent molecular area for at least 5 min. In order to record the isotherm (Π-A) curves, the monolayer was then compressed at a rate upto 0.1 $nm^2 \cdot mol^{-1} \cdot min^{-1}$. The temperature in the trough was kept constant at 20 °C by external circulating water.

Fluorescence experiments

Fluorescence measurements were carried out on a Kontron SFM25 interfaced with an Apple IIe microcomputer for data collection and manipulation. The slits were set to 5 nm (excitation) and 10 nm (emission). Temperature control was by circulating water from a Huber waterbath through a four-cell holder in which the temperature was monitored by a thermocouple placed in a buffer-filled cuvette.

The fluorescence results are presented as the relative quantum yield (Φ) calculated as the integral between 400 and 520nm of the fluorescence emission spectrum. Emission wavelength is presented as the barycentre of the integral between 400 and 520 nm according to the equation:

$$\lambda_m = \frac{\sum F(\lambda) \times \lambda}{\sum F(\lambda)} \quad (1)$$

where λ_m = barycentric mean wavelength, $F(\lambda)$ is the point fluorescence at wavelength λ. Measurements were taken every 1 nm. All fluorescence experiments were carried out using 1 cm pathlength Suprasil cuvettes containing at least 2.5 ml of sample with an absorption at 364 nm of less than 0.1. Absorbance spectra were measured on a Beckman Du-8 or an LKB Biochrom spectrophotometer.

Results

Mixed monolayers of A21978C and DMPC

The monolayer characteristics of pure A21978C films spread on water and various salt solutions have already been studied [9]. The mixed monolayers were spread on 1 M saline subphases of either KCl, $CaCl_2$ or $MgCl_2$. Fig. 1 shows typical isotherm (Π-A) curves for the two pure components and for their mixtures at different molar fractions (x_a) of A21978C ((x_a = A21978C/(A21978C + DMPC); i.e., $x_a = 0$ in a pure DMPC monolayer). The isotherms of pure A21978C show a transition region as noted in our previous study [9]. The pressure at the beginning of the transition (Π_t) increases almost linearly with the amount of DMPC in the monolayer (see Fig. 1 insets for K^+ and Ca^{2+} subphases). This continuous variation of the transition pressure with composition indicates that A21978C and DMPC are at least partially miscible.

Data from the isotherms are shown as area-composition (A vs. x_a) plots in Fig. 2, where the dotted lines indicate the result of simple addition of fractional molecular areas [14]:

$$A_{12} = x_1 A_1 + x_2 A_2 \quad (2)$$

where A = mean molecular area, x = molar fraction, and the subscripts 1, 2, and 12 refer to pure components 1 and 2 and their mixture, respectively. Three graphs are shown for each subphase corresponding to the molecular areas obtained at 5, 15 and 25 $mN \cdot m^{-1}$. When a mixed monolayer is spread on 1 M KCl, the deviations from linearity are small at low pressure below the equimolar ratio ($x_a = 0.5$), but when the amount of antibiotic is increased, the deviations are negative. They become large and positive at a surface pressure (Π) = 15 $mN \cdot m^{-1}$ (about 40% at a mole fraction (x_a) = 0.67). On 1 M $MgCl_2$, the deviations are small and negative when $x_a < 0.5$ and the surface pressure is below 10 $mN \cdot m^{-1}$. Above this pressure the deviations become positive. Large negative deviations are observed when the monolayer is spread on 1 M $CaCl_2$, and this is reversed only when the surface pressure exceeds 25 $mN \cdot m^{-1}$, and the deviations then become positive for $x_a > 0.5$. These deviations of the A vs. x_a plots from linearity provide evidence of non-ideal mixing. The thermodynamics of these processes have been studied by calculating the excess free energy change upon mix-

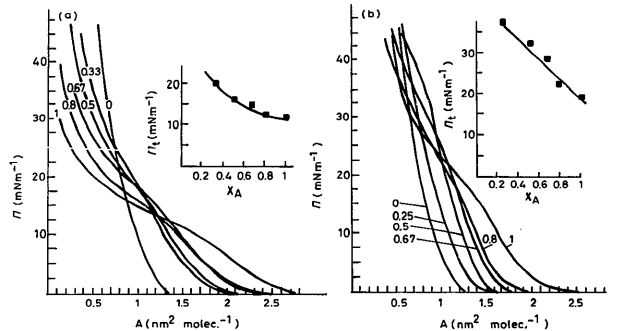

Fig. 1. Surface pressure-mean molecular area isotherms for mixtures of A21978C and DMPC. Encircled figures on each isotherm are the molar fraction (x_a; see text). The subphase was 1 M KCl (a) and 1 M $CaCl_2$ (b). Insets show the transition pressure Π_t vs. x_a of A21978C. The temperature was 20 °C.

ing above that found for an ideal mixed monolayer, using the relationship described by Goodrich [15]:

$$\Delta G_m^{ex} = \int_0^{\Pi} A_{12} d\Pi - x_1 \int_0^{\Pi} A_1 d\Pi - x_2 \int_0^{\Pi} A_2 d\Pi \quad (3)$$

The values of ΔG_m^{ex} were obtained by integrating under the Π-A curves of the mixture and of each of the pure components. The upper limit of integration was the surface pressure at the end of the transition on the isotherm curves of pure A21978C (18 mN · m^{-1} when spread on KCl, 22 mN · m^{-1} on $MgCl_2$ and 30 mN · m^{-1} on $CaCl_2$). Positive values of ΔG_m^{ex} indicate that the interactions between the pure component molecules themselves are stronger than interspecies or 'mutual' interactions. On the other hand, negative values of ΔG_m^{ex} are proof of specific interactions between the two components that increase the stability of the monolayer. The results are shown in Fig. 3a.

When the mixed monolayer is spread on 1 M KCl, the excess free energy change is mostly positive but its value decreases continuously as the amount of antibiotic increases. When the monolayer is spread on $MgCl_2$ 1

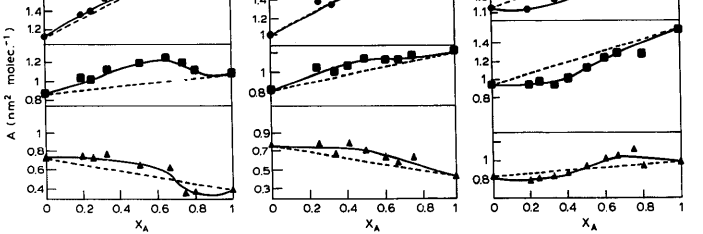

Fig. 2. Mean molecular area as a function of mole fraction of A21798C at different surface pressures, ●, 5 mN·m^{-1}; ■, 15 mN·m^{-1}; ▲, 25 mN·m^{-1}. The subphase was (a) 1 M KCl; (b) 1 M $MgCl_2$; (c) 1 M $CaCl_2$. The temperature was 20 °C.

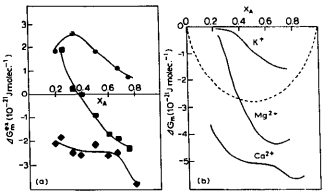

Fig. 3. Thermodynamic properties of A21978C and DMPC mixed monolayers. (a) Excess free energy of mixing as a function of monolayer composition. The subphase was ● 1 M KCl; ■, 1 M $MgCl_2$; ◆, 1 M $CaCl_2$. The temperature was 20 °C. (b) Total free energy of mixing as a function of monolayer composition; — — — corresponds to the values expected from an ideal mixture.

M, ΔG_m^{ex} is positive for small values of x_a and decreases continuously so that negative values occur for $x_a > 0.4$. This shows that the interactions of A21978C with DMPC become greater when there are more than two antibiotic molecules per three DMPC molecules.

The behaviour of mixed antibiotic-DMPC monolayers is quite different when spread on 1 M $CaCl_2$. The values found for ΔG_m^{ex} are negative over the whole range of composition, with a minimum corresponding to a high antibiotic : lipid ratio (at least $x_a > 0.8$). This shows that on $CaCl_2$ subphases A21978C interacts strongly with DMPC at all ratios. Now let us consider the total free energy change ΔG_m:

$$\Delta G_m = \Delta G_m^{ex} + \Delta G_m^{id} \quad (4)$$

$$\Delta G_m^{id} = kT(x_1 \ln x_1 + x_2 \ln x_2) \quad (5)$$

(ΔG_m^{id} is the free energy change for an ideal mixture, k = Boltzman's constant, T is the absolute temperature) [14]. In all cases ΔG_m was found to be negative over the whole range of mole fractions. This indicates that the mixed antibiotic-phospholipid monolayers are thermodynamically more stable than the monolayers of the pure components.

Fluorescence measurements in vesicles

The Kynurenine fluorescence of all A21978C variants (C10, C11, C12, C13) was measured in DMPC vesicles with respect to two factors. Firstly, their response to the lipid phase transition and secondly, their relative fluorescence quantum yields as a function of calcium ion concentration. In all the experiments the fluorescence yield declined with increasing temperature due to increased non-radiative losses. Fig. 4 shows a series of results obtained with A21978C12. In aqueous solution C12 emission shows an almost linear decline which is accompanied by a very small change in emission wavelength.

In DMPC vesicles without calcium ions this fall in yield with temperature is much greater than in aqueous solution (although the relative quantum-yield is always higher in the vesicle suspensions [8]). This is accompanied by a clear red-shift in the emission wavelength which, although more marked around the lipid phase transition, occurs over the whole temperature range. At the lipid phase transition there is a slight increase in yield which is not seen in experiments using the shorter chain length LY146032 [8]. This was the only clear difference noted between the various chain length versions. In the presence of DMPC and calcium ions the fluorescence decline is similar to that in aqueous solution until the phase transition temperature is reached, when the yield increases significantly as found previously [8]. Using the precise measure of emission wavelength, this rise in yield was seen to be accompanied by a blue shift.

Hence, at temperatures below the lipid phase transition, the difference in λ_m between zero $CaCl_2$ and 50

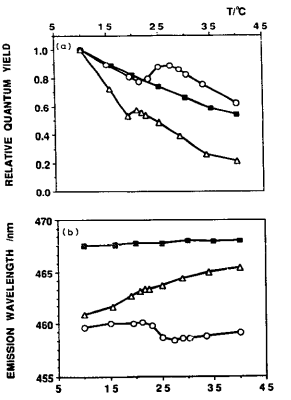

Fig. 4. Temperature dependence of the fluorescent yield and emission wavelength of the Kyn residue of A21978C. 10^{-5} M A21978C was mixed with (■) standard buffer, (○) standard buffer + 1 mg/ml DMPC vesicles, (△) standard buffer + 1 mg/ml DMPC vesicles + 50 mM $CaCl_2$, at 10 °C. The temperature was then increased stepwise, with fluorescence spectra being recorded at the points shown. Each point is the mean of three measurements. (a) Relative quantum yield of Kyn calculated as described in the text and normalised to a value of 1.0 at 10 °C. (b) Barycentric maximum emission wavelength calculated as described in the text.

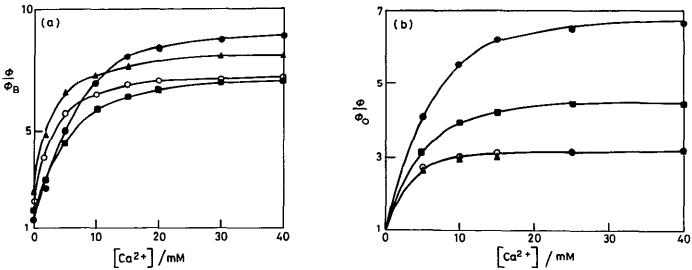

Fig. 5. Effect of lipid tail size on the calcium-dependent fluorescence enhancement. Samples of A21978C at a nominal concentration of $5 \cdot 10^{-6}$ M in standard buffer were adjusted to the same absorbance at 255 and 360 nm. Their fluorescence was measured and the relative quantum yield taken to equal Φ_B (the yield in buffer). 1 mg/ml egg-PC SUVs were added and the fluorescence Φ (expressed as Φ/Φ_B) increased to the values shown at zero $[Ca^{2+}]$ in part (a). The $[Ca^{2+}]$ was increased by the addition of $CaCl_2$ from concentrated stock and the Φ was then measured. Part (b) shows the result of normalising to a value of one, all the Φ values at $[Ca^{2+}] = 0$. Here the yield is expressed as Φ/Φ_0; (the yield at $[Ca^{2+}] = x$ mM)/(the yield at $[Ca^{2+}] = 0$ mM) and is an expression of the relative calcium sensitivities. Temperature = 20 °C. λ excitation = 365 nm. ●, C10; ■, C11; ○, C12; ▲, C13.

mM $CaCl_2$ samples is 1.3 nm, whilst at 30 °C it has increased to 5.8 nm. This is made up by a red-shift in the calcium free samples of 3.5 nm and a blue shift in the calcium containing samples of 1 nm. These wavelength measurements clearly indicate that what we see as a calcium-induced increase in emission above the phase transition is the result of two factors. Firstly, the blue-shift and increase in emission in the presence of calcium which clearly indicates an increased interaction between the antibiotic and the vesicles above the phase transition. Secondly, the red-shift occurring in the absence of calcium shows that under these conditions the antibiotic–membrane interaction weakens above the phase transition.

The effect of increasing calcium concentration on the Kyn fluorescence in DMPC vesicles, previously determined solely for the C10 derivative [8], was measured for the other members of the A21978C series (Fig. 5). The samples of peptide were adjusted to give the same absorbance at 255 and 360 nm (two absorption bands of Kyn) and their fluorescence yields measured first in the absence of SUVs. Relative to C10, the values of the fluorescence yields were 0.92 (C11), 1.08 (C12) and 1.03 (C13). These values were used as Φ_B in calculating the quantity Φ/Φ_B (fluorescence yield in PC vesicles/fluorescence yield in buffer). On adding concentrated vesicles and allowing for the subsequent dilution of the peptide, all the samples showed an increase in yield. This increase occurred in the order C13 > C12 > C11 > C10. As polarisation experiments have previously shown C10 to be fully bound under these conditions, this increase in yield with increasing chain length is evidence that the larger hydrophobic region causes a closer approach of the Kyn residue to the membrane (Fig. 5a) rather than an increase in bound peptide. This situation does not persist in the presence of calcium ions as the C10 version increases in yield more quickly than the others and is the most fluorescent above 12 mM $CaCl_2$. On replotting the data with Φ_0 (fluorescence yield at $Ca^{2+} = 0$) instead of Φ_B as the starting fluorescence, this apparent anomaly is shown to be part of a general trend towards greater calcium sensitivity with decreasing chain length.

Discussion

We have previously shown that A21978C binds to lipid bilayer membranes initially through its lipid moiety, and that the presence of calcium ions probably causes a deeper penetration of the headgroup into the lipid bilayer [8]. Both fluorescence [8] and monolayer [9] methods have shown that a calcium-selective site exists on the peptide itself, and in the latter a calcium specific conformational change was demonstrated. Two features of this interaction remained unresolved. First: are there specific interactions between A21978C and phospholipids? And secondly: what are the relative contributions of calcium and the lipid tail to the membrane interaction? The results presented here demonstrate a specific interaction between A21978C, Ca^{2+} and DMPC, and illustrate its subsequent effects on the membrane binding provoked by the fatty acyl tail.

The monolayer results provide direct information about how the antibiotic interacts with DMPC. The dependence of the transition pressure, Π_t, upon the

amount of A21978C in the monolayer and the deviation from linearity of the area vs. composition plots are consistent with at least a partial miscibility of the two peaks at the air/water interface. The quality of the mixing is, however, closely related to the cation composition of the subphase.

By examining the sign of the excess free energy change we can gain a clearer idea of the strengths of the various interactions occurring within the mixture. Indeed, this parameter can be considered as a measure of the spontaneous tendency of the two molecular species to mutually interact, and it shows clearly the differences between the mixtures spread over KCl, $MgCl_2$ and $CaCl_2$ subphases. On a KCl subphase, the positive values of ΔG_m^{ex} vs. mole fraction plots show that antibiotic–DMPC interactions are weaker than antibiotic–antibiotic or lipid–lipid interactions. This means that the antibiotic molecules will have a tendency to self-associate, forming perhaps antibiotic-rich patches. However, the antibiotic-DMPC mixed monolayers are always more stable than the unmixed ones since the total free energy change ΔG_m is negative over the whole range of monolayer composition. Thus we can conclude that phase segregation in the monolayer is unlikely. On $MgCl_2$ subphases the antibiotic and lipid molecules begin to interact only at a mole fraction of 0.4, and privileged interactions occur at an antibiotic : DMPC molar ratio of 2 : 1. On $CaCl_2$ subphases, A21978C is always associated with DMPC, with a more specific complex being formed at high antibiotic to lipid ratios.

Hence, the DMPC–antibiotic interactions are significant only in the presence of calcium. It was shown previously that a calcium specific site exists on the peptide and that binding of Ca^{2+} provokes a conformational change [8,9]. The evidence presented here indicates that Ca^{2+} plays a role in inducing strong antibiotic–phospholipid interactions. However, the antibiotic-DMPC complex formed at high antibiotic concentrations seems unlikely to be applicable to the calcium dependence of the antibacterial activity. Rather, it is the large differences in lipid interactions provoked by the various ions at low antibiotic mole fractions that appear to have most in common with the results in vesicles and in vivo.

The interaction with vesicles has been further studied by following the fluorescence of the Kyn residue which, combined with the calculation of the barycentric mean emission wavelength (λ_m), clarified the behaviour of the peptide during the lipid phase transition. The unexpected result was that the fluorescence of the peptide bound to the membrane in the absence of calcium showed an increased temperature sensitivity compared to the free peptide in solution. The analysis of emission wavelength showed that this was associated with a red-shift and hence a move into a less hydrophobic environment. One explanation for this could be the negative change in surface potential (ψ) that is thought to accompany the phase transition [16]. Hence, when ψ becomes more negative, the A21978C molecule is repelled from the surface, causing a red-shift. The increase in temperature may also increase the solvent exposure of the Kyn residue through an increase in the surface area per polar headgroup of the DMPC [17,18]. If the calcium-bound form is buried deeper in the membrane, then such effects will be lessened. Thus the increase in wavelength difference between the two forms above the phase transition has two likely components. Firstly, a deeper penetration of the bilayer by the calcium form at the phase transition. Secondly, a greater temperature dependence of the calcium-free form which may reflect an increased solvent exposure and molecular mobility at the bilayer surface. Similar effects have been seen using ANS in distearoyl-PC membranes [19].

Although the overall behaviour of the various versions is similar, the chain length exerts an influence on the magnitude of the calcium-induced fluorescent enhancement. In the absence of Ca^{2+} we obtained the not unexpected result that the relative quantum yield increases with lipid chain length. Hence the probable average distance of the Kyn from the bilayers hydrophobic core decreases in the order C10 > C11 > C12 > C13. This is not a partitioning effect, as C10 appears completely bound to vesicles under these conditions [8]. The subsequent reversal of this state of affairs provides strong evidence that the calcium effect itself is actually inhibited by a long lipid chain. It is not possible to say whether this is due to prevention of a conformational or orientational change in the membrane by the fatty tail, but clearly in 50 mM $CaCl_2$ the Kyn residue of the C10 version is in a less polar environment than that of C13. The important conclusion from this result is that the specific interaction seen in the monolayers is not a hydrophobic-hydrophobic liaison aided by the effect of the bound calcium as a charge neutraliser. The interaction is actually enforced by the polar heads of both molecules and the lipid tail appears to be most important in the initial attachment of the antibiotic to the membrane.

In summary, we have shown that these antibiotics have specific interactions with phospholipids in the presence of calcium ions and that these interactions are probably strongest at the polar headgroups. Such data will help to explain the type of membrane interaction that plays a role in the activity of this antibiotic.

Acknowledgements

J.H.L. is currently an EMBO postdoctoral fellow and also wishes to thank the SERC (U.K.) for the award of a Nato postdoctoral fellowship which enabled him to work at the CBM Orléans. The technical assistance of M. Charlier is gratefully acknowledged.

References

1 Eliopolous, G.M., Thaubin, C., Gerson, B. and Moellering, R. (1985) Antimicrob. Agents Chemother. 27, 357–362.
2 Debono, M., Barnhart, M., Carrell, C.B., Hoffman, J.A., Occolovitz, J.L., Abbott, B.J., Fukuda, D.S., Hamill, R.L., Biemann, K. and Herlihy, W.C. (1987) J. Antibiot. 40, 761–777.
3 Allen, N.E., Hobbs, J.N. and Alborn, W.E. (1987) Antimicrob. Agents Chemother. 31, 1093–1099.
4 Maget-Dana, R., Heitz, F., Ptak, M., Peypoux, F. and Guinand, M. (1985) Biochem. Biophys. Res. Commun. 129, 965–971.
5 Bannerjee, D.K., Scher, M.G. and Waechter, C.J. (1981) Biochemistry 20, 1561–1568.
6 Stone, J.K. and Strominger, J.L. (1971) Proc. Natl. Acad. Sci. USA 68, 3223–3227.
7 Storm, D.R., Rosenthal, K.S. and Swanson, P.E. (1977) Annu. Rev. Biochem. 46, 723–763.
8 Lakey, J.H. and Ptak, M. (1988) Biochemistry 27, 4639–4645.
9 Maget-Dana, R., Lakey, J.H. and Ptak, M. (1988) Biochim. Biophys. Acta 962, 201–207.
10 Lakey, J.H., Maget-Dana, R. and Ptak, M. (1988) Biochem. Biophys. Res. Commun. 150, 384–390.
11 Singleton, W.S., Gray, M.S., Brown, M.L. and White, J.L. (1965) J. Am. Oil. Chem. Soc. 42, 53–56.
12 Chen, P.S., Toribara, T.Y. and Warner, H. (1956) Anal. Chem. 28, 1756–1758.
13 Harnois, I., Maget-Dana, R. and Ptak, M. (1988) J. Colloid. Interface Sci. 123, 85–88.
14 Gaines, G.L., Jr. (1966) in Insoluble monolayers at liquid gas interfaces, p. 136–207, Interscience, New York.
15 Goodrich, F.C. (1957) in Proceedings of the 2nd International Congress of Surface Activity, Vol. 1, p. 85, Academic Press, New York.
16 Tatulian, S.A. (1987) Biochim. Biophys. Acta 901, 161–165.
17 Radda, G. and Vanderkooi, J. (1973) Biochim. Biophys. Acta 265, 509–549.
18 Gulik-Kryzwicki, T., Schechter, E., Iwatsubo, M., Ranck, J.L. and Luzzati, V. (1970) Biochim. Biophys. Acta 219, 1–10.
19 Trauble, H. and Overrath, P. (1973) Biochim. Biophys. Acta 307, 491–496.